Appl. Phys. B 78, 137–144 (2004)
DOI: 10.1007/s00340-003-1304-6

Applied Physics B
Lasers and Optics

A. WICHT[1,✉]
M. RUDOLF[2]
P. HUKE[2]
R.-H. RINKLEFF[2]
K. DANZMANN[2,3]

Grating enhanced external cavity diode laser

[1] Institut für Experimentalphysik, Heinrich-Heine-Universität Düsseldorf, Universitätsstr. 1, 40225 Düsseldorf, Germany
[2] Institut für Atom- und Molekülphysik, Universität Hannover, Callinstr. 38, 30167 Hannover, Germany
[3] Max-Planck-Institut für Gravitationsphysik, Callinstr. 38, 30167 Hannover, Germany

Received: 1 June 2003/Revised version: 7 August 2003
Published online: 27 November 2003 •

ABSTRACT We describe a concept for diode lasers with optical feedback. It is based on the combination of two different diode laser concepts: the diode laser with (i) feedback from a grating and (ii) resonant optical feedback from a separate cavity. The goal of our work is to unite the excellent tunability and well known reliability of grating diode lasers with the narrow emission linewidth of diode lasers with resonant optical feedback. Our theoretical description shows that a proper cavity design is essential for this concept. It also provides the means to optimize the cavity geometry. Our setup is based on an AR-coated laser diode emitting at 852 nm. It achieves an overall tuning range of 36.4 nm and a continuous tuning range of 45.1 GHz. A beat note measurement with a diode laser with resonant optical feedback demonstrates a short-term linewidth below 60 kHz. Continuous tuning ranges on the order of nanometers and linewidth on the order of kHz seem feasible.

PACS 42.55.Px, 42.60.By, 42.40.Eq

1 Introduction

Diode lasers have become an important tool in the fields of quantum optics, especially for laser spectroscopy. They are relatively cheap and reliable sources of coherent radiation [1, 2]. With a selection of different laser diodes one can basically cover the whole range of the optical spectrum from the blue [3] to the far infrared [4]. Diode lasers based on single transverse mode laser diodes provide large modulation bandwidth [5], large continuous tuning ranges [6] and narrow linewidth emission [7].

In order to reduce the emission linewidth of diode lasers two different approaches to "self-injection-locking" have been developed: Fleming and Mooradian [8] first used an optical grating to feed a fraction of the light emitted by the laser diode back into its active region. Because in this setup the cavity is typically extended by a grating, we will call this setup the *extended* cavity diode laser setup. The feedback reduced the short-term linewidth of the laser to 1.5 MHz. In general, the linewidths of extended cavity diode lasers range from 100 kHz to MHz depending on the type of the laser diode [1]. Shortly after Fleming and Mooradian, Dahmani et al. [9] employed resonant optical feedback from a separate cavity to reduce the short-term linewidth even further to the level of a few kHz. As this setup uses a "separate" cavity, which is external to the diode laser cavity, we will call this type of setup an *external* cavity diode laser. Please note that there is confusion in the literature about the wording for the different types of diode laser setups.

Both approaches lead to complementary results: diode lasers with optical feedback from a cavity provide the smallest linewidth. For these lasers the frequency noise at large Fourier frequencies is strongly reduced. They are therefore well suited for applications where e.g. two independent lasers have to be phase locked by means of an optical phase locked loop. However, their continuous and over all tuning ranges are much smaller than those of extended cavity diode lasers due to the lack of an "intra-cavity" element that provides a coarse wavelength pre-selection. Further, extended cavity diode lasers are much easier to use and are more reliable than external cavity diode lasers. For example, extended cavity diode lasers show much better frequency repeatability than external cavity diode lasers that usually require four dependent actuators to set the wavelength: i.e. the current, an etalon, the length of the feedback cavity, and the position of a mirror used to adjust the path length to the external cavity. For an extended cavity diode laser there are only two actuators (current, grating), which are almost independent, if only modest tuning ranges (∼GHz) have to be achieved.

There have been efforts to connect both ideas to combine the advantages of both approaches and to overcome the drawbacks. For example, Hayasaka [10] and Patrick and Wieman [11] added optical feedback from an external cavity to an extended cavity diode laser. The light was injected and fed back via the 0th-order output of the grating. In this setup two feedback channels compete with each other via a strongly non-linear interaction (mediated by the diodes active medium) which is a hard-to-control situation. Further, the external cavity also feeds back at those frequencies that are different from the selected frequency.

In this paper we describe an approach that truly combines the external cavity and the extended cavity setup. The basic idea is to use an extended cavity diode laser with the 1st order diffraction field of the grating being injected into an external cavity (*grating enhanced external cavity diode laser*, GEECDL). We present a theoretical analysis aimed at finding

✉ Fax: +49-211/8113116, E-mail: Andreas.Wicht@uni-duesseldorf.de

the optimum cavity geometry. Further, experimental results are given for a comparison between three different types of cavities, which are favored by our theoretical description. We investigate the continuous and overall tuning ranges of our GEECDLs, which all employ AR-coated laser diodes. Finally, we discuss the results of a linewidth measurement based on measuring the beat note between the new setup and an additional external cavity diode laser. It should be mentioned that the same experimental approach has been considered in [12] independently from us.

We would like to point out again, that our aim is to develop a guideline for choosing the optimum cavity geometry rather than to present a complete analysis of the dynamic properties of the laser system. Hence, a very simplified model serves for our purpose, which is based on geometrical optics only and which does not include many important effects in semiconductor lasers [13]. Belenov et al. [14] discussed a very similar type of setup within their theoretical analysis of the linewidth displayed by different diode lasers systems that are subject to optical feedback.

2 Basic idea and problems

The basic idea of the new setup is to overcome the shortcomings related to external cavity diode lasers by adding an element to the setup that allows for a coarse frequency preselection. Hence, it seems natural to replace one of the mirrors between the laser diode and the external cavity by an optical grating. An alternative but equivalent point of view is starting from the Littman configuration, see Fig. 1, in which the 1st order diffraction output of the desired wavelength is retro reflected back to the laser diode. In order to achieve the narrow linewidth known from external cavity diode lasers it seems straightforward to replace this retro mirror by the same folded cavity that is used for external cavity diode lasers (see Fig. 3).

In order to point out the basic problem our approach has to solve we briefly focus on the Littman setup, Fig. 1. If the wavelength does not match the selected wavelength, then the grating and the mirror will introduce a translational and angular separation (angle γ) between the beam emitted by the laser diode and the corresponding retro-diffracted beam. Due to the good collimation of the laser beam by the diode laser collimating lens the mode mismatch between both of these beams is almost solely defined by their angular separation. It can be shown that any experimentally realistic translational separation of the beams does not significantly affect the mode mismatch and can be neglected. This outlines the general strategy behind our theoretical analysis: any potentially interesting cavity replacing the retro mirror in Fig. 1 must, at least maintain the angular separation between the retro-diffracted beam at the selected wavelength λ_0 and an equivalent beam at some detuned wavelength $\lambda' = \lambda_0 + d\lambda$. Please note that according to our discussion above this angular separation has to be measured between the collimating lens and the grating. A specifically "bad" example would be a regular Littman setup with a concave mirror placed at a distance from the grating, which equals the mirrors radius of curvature. In this case, all beams are exactly retro-diffracted into the emitted mode regardless of their wavelength so that the curved mirror cancels the dispersion of the grating.

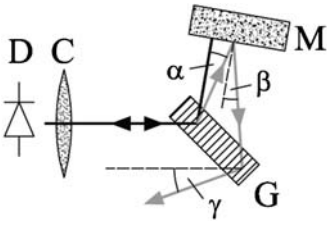

FIGURE 1 Littman laser setup. *D*: laser diode, *C*: collimating lens, *G*: transmission grating. The ray corresponding to a specific wavelength λ_0 is retro-reflected by mirror *M*. Rays corresponding to a different wavelength λ' will be at angle α with respect to the ray at λ_0 after first diffraction, at angle β after reflection by mirror *M* and at angle γ after second diffraction by the grating

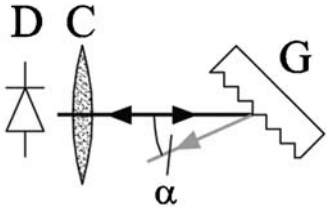

FIGURE 2 Littrow laser setup. *D*: laser diode, *C*: collimating lens. For a specific wavelength λ_0 the beam is retro-diffracted by grating *G*. For a different wavelength λ' the emitted and diffracted beams are angularly separated by angle α

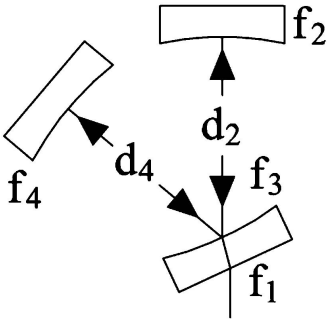

FIGURE 3 Optical feedback cavity. The input coupler has focal length $f_1 = \infty$ upon transmission and f_3 upon reflection inside the cavity. A folded cavity design is necessary in order to avoid direct feedback from mirror f_1

3 Cavity geometry

Our analysis starts with the Littrow laser setup, see Fig. 2. We follow two rays emitted at wavelength λ_0 and $\lambda' = \lambda_0 + d\lambda$. Let us assume that the ray at λ_0 satisfies the Littrow condition and hence is retro-diffracted onto itself. The diffracted ray at λ' does not meet the Littrow condition and therefore is at an angle α with respect to the ray at λ_0. Due to this mode mismatch there is stronger feedback for the ray at λ_0 so that the grating selects λ_0 as the operating wavelength.

Now consider the Littman laser setup shown in Fig. 1. The two rays at λ_0 and λ' are angularly separated by the angle α upon first diffraction by the grating (we assume a transmission grating here, see Sect. 4). While the ray at λ_0 is exactly retro-reflected the ray at λ' will be at an angle β with respect to the ray at λ_0. In the case of a Littman laser $\beta = \alpha$. However, in the general case of a complex cavity replacing the mirror, β will be a function of α and of the spatial separation x between the two reflection points at the surface of the mirror (see Fig. 1 and Fig. 3). If we neglect dispersion effects of the cavity, β does not depend on the wavelength attributed to the ray

so that $\beta = \beta(\alpha, x)$. We continue to follow the ray propagation and recognize that the ray at wavelength λ' is diffracted towards the laser diode upon second traversal through the grating. Hence, it finally is at an angle γ with respect to the ray emitted by the laser diode. As long as $|\gamma| \geq |\alpha|$ the combination of grating and mirror or cavity provides the same spectral selectivity as the Littrow setup.

For the sake of simplicity let us always assume that the distance between the grating and the mirror/cavity is negligibly small. Further, for the case of the mirror being replaced by a cavity, let us for now assume that the ray at λ_0 is injected on the axis of the cavity so that it is always retro-reflected. Consequently, the ray at λ' will be injected *at* but not parallel to the axis of the cavity. The reflection of the ray at λ' is therefore described by $\beta(\alpha, x = 0)$. Applying the *ABCD*-formalism [15] one can show that $|\gamma| \geq |\alpha|$ is equivalent to $\left|\left[\partial_{\Theta_{IN}} \Theta_{OUT}\left(\Theta_{IN}, \lambda'\right)\right]^{-1} \cdot [\partial_\alpha \beta + 1]\right| \geq 1$. Here, Θ_{IN} and Θ_{OUT} are the angles between the normal to the physical plane of the grating and the incoming and outgoing ray, respectively. Please note that in the paraxial limit $\beta(\alpha, x)$ is linear in α and x and $\partial_\alpha \beta(\alpha, x) = \partial_\alpha \beta$ is a constant, i.e. independent of α and x. For optical gratings with typical line densities of 1600 l/mm for $\lambda_0 = 852$ nm we find $\left[\partial_{\Theta_{IN}} \Theta_{OUT}\left(\Theta_{IN}, \lambda'\right)\right]^{-1} \approx 1$ so that $|\gamma| \geq |\alpha|$ can be stated in the form

$$\partial_\alpha \beta(\alpha) \notin -2...0\ . \tag{1}$$

This is our fundamental requirement. If this equation is not satisfied, then $|\gamma| < |\alpha|$. Consequently, the spectral selectivity of the system consisting of the grating and the mirror/cavity is reduced with respect to the corresponding Littrow setup. This may result in multimode or unstable laser operation. For a Littman setup one finds $\partial_\alpha \beta = +1$, which corresponds to $\gamma = 2\alpha$. From the geometrical optics point of view, the Littman setup obviously has a better spectral selectivity than the Littrow setup for which $\gamma = \alpha$. Of course, this is due to the reflection at the retro mirror, which doubles the angular separation between incident and excident ray.

Let us now replace the mirror of the Littman setup by the cavity shown in Fig. 3. Each of the successive round trips $n = 0, 1, ...$ of the ray at λ' inside the cavity generates a ray exiting the cavity with corresponding β_n and $\partial_\alpha \beta_n$. For a given cavity geometry the goal now is to calculate all $\partial_\alpha \beta_n$ for $n = 0, 1, ...N$, where N is the number of effective round trips determined by the cavity finesse. A specific cavity geometry is considered useful only if none of the $\partial_\alpha \beta_n$ with $n = 0...N$ lies within the band of width 2 centered on -1, which is specified by (1).

As an example for our analysis procedure we pick a specific resonator, say $f_1 = f_3 = \infty$ (planar input coupler) and $f_2 = f_4 = f$ and choose the length of both parts of the cavity to be equal: $d_2 = d_4 = D/2$. D gives the dimension of the cavity and in this example equals the overall cavity length. Obviously, the ratio of the cavity dimension D to the focal length f determines the cavity geometry. Hence, to describe the geometry by a single number, we define the geometry factor

$$\epsilon = \frac{D}{4f}\ . \tag{2}$$

As we vary ϵ from 0 to 1, we change the resonator geometry from planar ($\epsilon = 0$) to "confocal" ($\epsilon = 0.5$) and finally to the "concentric" geometry at $\epsilon = 1$. It should be noted that the range $\epsilon = 0...1$ covers all stable resonators of this geometry class.

For each individual value of ϵ we calculate $\partial_\alpha \beta_n$ for $n = 0...25$ meaning that we assume a finesse for the cavity, which does not exceed $\mathcal{F} \sim 150$. This is well satisfied for our experiment ($\mathcal{F} \sim 50...100$). The result of the calculation is given as a plot of $\partial_\alpha \beta_n$ *vs.* ϵ, see Fig. 4. For the sake of clarity, only $n = 0...10$ is shown. The shaded area denotes the "forbidden" range $-2...0$ of $\partial_\alpha \beta_n$ as determined by (1). Obviously, $\epsilon = 0.5$ corresponding to a confocal resonator is a promising geometry. This is also true for the planar resonator $\epsilon = 0$ which is not obvious from Fig. 4.

We focus at the confocal geometry now and find the result given in Fig. 5. In this graph, $\partial_\alpha \beta_n$ is shown for a selection of round trips n between $n = 0$ (direct reflection from mirror with focal length f_2) and $n = 25$. For this confocal setup (1) is satisfied only if the geometry actually is *exactly* confocal, i.e. $\epsilon \equiv 0.5$. However, from an experimental point of view it is impossible to exactly realize a specific geometry (e.g. distance between mirrors). By replacing (1) by

$$\partial_\alpha \beta_n \notin -1.9... - 0.1 \tag{3}$$

we barely relax our fundamental requirement but we now are able to identify a certain range $\Delta\epsilon$ for the cavity geometry factor ϵ, which provides a wavelength selectivity essentially identical to that of the Littrow setup. The slightly relaxed requirement and the corresponding potentially useful geometry range are marked by the shaded area in Fig. 5. According to (2) a geometry range of $\Delta\epsilon \approx 1.9 \times 10^{-3}$ corresponds to $\Delta D = 4 f \Delta\epsilon$, which amounts to $\Delta D = 0.29$ mm for $f = 37.5$ mm as in our experiment. The geometry range $\Delta\epsilon$ is later used to estimate and compare the performance of different geometries that meet the relaxed fundamental requirement (3).

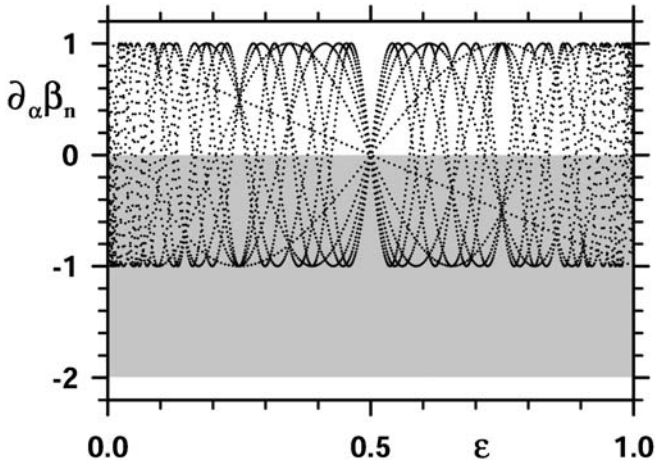

FIGURE 4 $\partial_\alpha \beta_n$ vs. cavity geometry factor ε for $n = 0..10$ and $f_1 = f_3 = \infty$, $f_2 = f_4 = f$. $\varepsilon = 0, 0.5$, and 1 correspond to planar, confocal, and concentric geometry, respectively. The geometries described by those ε, for which no $\partial_\alpha \beta_n$ is found within $-2 \ldots 0$ are potentially useful, e.g. $\varepsilon = 0.5$. The "forbidden" range $-2 < \partial_\alpha \beta_n < 0$ is depicted by the *shaded area*

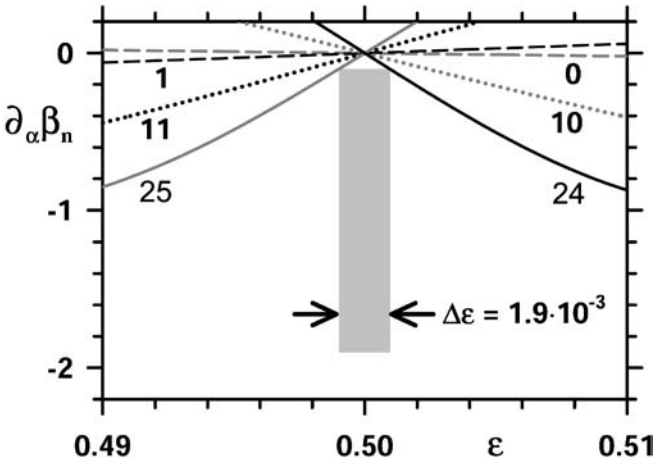

FIGURE 5 $\partial_\alpha\beta_n$ vs. cavity geometry factor ε for $f_1 = f_3 = \infty$ and $f_2 = f_4 = f$ in the vicinity of the confocal geometry $\varepsilon = 0.5$. $\partial_\alpha\beta_n$ is shown for a selection of different values of n between 0 and 25. The shaded range of width $\Delta\varepsilon$ (height: $-1.9\ldots-0.1$) is free of any curves $\partial_\alpha\beta_n$ and therefore is likely to provide stable laser operation

Next we want to develop two more criteria that are useful to compare different cavity geometries. An experimental realization of the GEECDL will always be affected by thermal drifts of one part of the setup with respect to the other. In particular, the external cavity may tilt with respect to the laser beam and drift transversely with respect to it. A tilt necessarily affects the operating wavelength of the GEECDL. However, the effect of a transverse displacement might be suppressed by proper resonator design: for a specific resonator under discussion we check, whether

$$\partial_x\beta_n = 0 \tag{4}$$

is satisfied for $n = 0...25$. If so, the angle γ between the emitted and reflected ray in Fig. 1 and hence the operating wavelength of the GEECDL are not affected by a potential transverse displacement of the cavity.

The second additional criterion is concerned with efficiently coupling the well collimated laser diode beam to the external cavity. This is an important issue, as a significant feedback level provides a large tuning range and a reliable and stable single mode operation of the laser. However, as long as the cavity geometry is not very close to a planar geometry, the collimated laser diode beam size (~ 1 mm) is much bigger than the beam size of the cavity modes at the input coupler (typically $\sim 200\,\mu$m for $\lambda = 850$ nm and mirror focal lengths of $f = 5$ cm). Hence, significant mode matching cannot be achieved without additional lenses placed between the grating and the input coupler of the cavity. These lenses would increase the size of the setup thereby potentially reducing the mechanical stability and possibly causing additional optical feedback to the laser diode. They should therefore be avoided. It is now helpful to recognize that specific geometries like the planar $\epsilon = 0$, the confocal $\epsilon = 0.5$, the concentric $\epsilon = 1$ as well as the geometries designated by $\epsilon = 0.25$ and $\epsilon = 0.75$ show a large gaussian mode degeneracy. Hence, even if the collimated laser diode beam cannot be mode matched to the *fundamental* mode of the cavity, significant coupling can still be achieved if one of the geometries $\epsilon = 0, 0.25, 0.5, 0.75$, or 1 is chosen.

To conclude, we now have three criteria at hand for the comparison of different resonator geometries: our relaxed fundamental requirement (3), the invariance of the operating wavelength under transverse displacement of the cavity (4) and cavity coupling criterion discussed above. We are now ready to investigate seven different classes of resonator geometries that are given in Table 1. In total we find are a few hundred geometries that satisfy the relaxed fundamental requirement (3). The next requirement is for a given geometry to be of one of the types ϵ=0, 0.25, 0.5, 0.75, or 1 for the reason already discussed above. This constraint reduces the number of potentially interesting geometries to eleven, which are explicitly given in Table 2.

Out of the eleven resulting geometries six are either planar ($\epsilon = 0$) or "concentric" ($\epsilon = 1$) geometries: these are 1, 2, 4, 8, 10, and 11. They are placed right at the stability boundary of optical resonators, which means that the size and position of the resonator modes is most strongly affected by inevitable misalignment of the mirrors due to thermal drifts etc. [16]. Since our goal is to find a setup, which is as reliable and as easy to use as a Littrow laser, these geometries are unfavorable. Hence, five interesting geometries are left, i.e. 3, 5, 6, 7, and 9. We next compare the width of the operating range $\Delta\epsilon$ among these five geometries. The smallest value is due to geometry 6, and corresponds to $\Delta D = 0.2$ mm for a typical focal length of $f_2 = f_4 = 5$ cm. This is an estimate for the accuracy that is required for setting the length of the cavity. As even this tight requirement is not too hard to achieve, all five geometries should be feasible experimentally. The largest operating range is due to geometry 3, and corresponds to $\Delta D = 3.8$ mm for the same focal length! Even more remarkably, this geometry is also unique in that it is the only setup among the remaining five geometries, which is not affected by a transverse displacement (e.g. drift) of the cavity with respect to the injected laser diode beam. Next, it is worth noting that among the five remaining geometries the confocal geometry 5 provides the largest degree of transverse gaussian mode degeneracy. Hence, it is likely to provide the strongest feedback among these geometries. Although its geometry range $\Delta D = 0.38$ mm is smaller than the corresponding range for the geometry 3 by a factor of 10, it is still big enough not to pose a technical problem.

class	f_2	f_3	f_4	d_2	d_4
1	f	f	f	D	D
2	∞	f	f	$D/2$	D
3	f	∞	f	$D/2$	$D/2$
4	f	f	∞	D	$D/2$
5	f	∞	∞	$D/4$	$D/4$
6	∞	f	∞	$D/2$	$D/2$
7	∞	∞	f	$D/4$	$D/4$

TABLE 1 Seven different classes of cavity geometries have been analyzed. The case $f_2 = f_3 = f_4 = \infty$ is included in each of the classes by setting $\varepsilon = 0$. d_2 and d_4 were chosen such that $\varepsilon = 0\ldots1$ covers the whole range of stable resonators of that specific geometry class and $\varepsilon = 0$, and 1 correspond to the planar and to the "concentric" geometry, respectively. For the meaning of f_i and d_i see Fig. 3

#	f_2	f_3	f_4	d_2	d_4	ε	$\Delta\varepsilon$	$\partial_x\beta_n$	note
1	∞	∞	∞	D	D	0	$8\cdot10^{-5}$	0	planar
2	$D/4$	$D/4$	$D/4$	D	D	1	$2.3\cdot10^{-4}$	$\neq0$	
3	∞	$D/3$	$D/3$	D/2	D	0.75	$1.9\cdot10^{-2}$	0	
4	∞	$D/4$	$D/4$	D/2	D	1	$4.2\cdot10^{-4}$	$\neq0$	
5	$D/2$	∞	$D/2$	D/2	D/2	0.5	$1.9\cdot10^{-3}$	$\neq0$	confocal
6	D	D	∞	D	D/2	0.25	$1.0\cdot10^{-3}$	$\neq0$	
7	$D/3$	$D/3$	∞	D	D/2	0.75	$3.6\cdot10^{-3}$	$\neq0$	
8	$D/4$	$D/4$	∞	D	D/2	1	$4.2\cdot10^{-4}$	$\neq0$	
9	∞	$D/3$	∞	D/2	D/2	0.75	$5.9\cdot10^{-3}$	$\neq0$	
10	∞	$D/4$	∞	D/2	D/2	1	$9.6\cdot10^{-4}$	$\neq0$	
11	∞	∞	$D/4$	D/4	D/4	1	$3.2\cdot10^{-3}$	$\neq0$	semi-concentric

TABLE 2 Theoretical analysis of seven classes of cavities according to Table 1. Out of all geometries, which satisfy the relaxed fundamental requirement (3), only those cavities are listed here that belong to one of the geometries $\varepsilon = 0, 0.25, 0.5, 0.75, 1$

In conclusion, our analysis suggests that geometries 3 and 5 are best suited for the realization of a GEECDL. The confocal geometry 5 is the least susceptible to inevitable mirror misalignment and provides the strongest coupling to the external cavity whereas geometry 3 provides by far the largest useful geometry range. The latter may be of importance for future setups employing high finesse external cavities. For these, the useful working range will be much smaller than the ranges discussed in this paper. For the experimental part of our work we focused on those geometries, which were accessible for us, i.e. the planar 1 the confocal 5 and the semi-concentric geometry 11. Geometries 1 and 11 are placed at the stability boundary. Hence, the experimental investigation of these three geometries provides a comparison of at-stability-boundary geometries to a geometry that is located at the center of the stability range.

Finally, we would like to mention again that geometry 1 has been realized by [12]. The authors also tried a "semi-confocal" and an almost planar geometry but were not able to achieve stable operation. The failure of these geometries is predicted by our model.

4 Experimental results

In this section we will first describe the experimental setup. Then, we will compare the performance of three different types of cavities mentioned in Table 2, i.e. the planar, the confocal, and the semi-concentric geometry. Finally, the results for a measurement of the beat note between the GEECDL and an external cavity diode laser will be presented. This provides the means to estimate the linewidth of the GEECDL emission.

4.1 *Experimental setup*

An index guided single mode laser diode was provided by *Sacher Lasertechnik* (SAL-850-50). At the maximum rated current of 120 mA it is specified to emit a power of 50 mW at the central wavelength of 865 nm. In order to reduce optical feedback, the front facet of the laser diode was AR-coated. With a residual reflectivity of $R = 3\cdot10^{-5}$ the threshold is 53.4 mA in the absence of optical feedback. Laser diodes of this type are routinely used by *Sacher Lasertechnik* for diode lasers in Littrow configuration and are typically tuneable within 830 nm–890 nm [17]. The light emitted by the laser diode is collimated by a *Geltech* C390TM-B AR-coated collimator ($f = 2.75$ mm, $NA = 0.65$). We use a holographic transmission grating provided by *STEAG ETA-Optik* with a line density of 1600 l/mm. It is placed at a distance of 20 mm from the collimator. At $\lambda = 852$ nm and with the polarization of the electric field oriented perpendicular to the plane of incidence the maximum diffraction efficiency for the 1st order is 65%. Approximately 5% of the input power is coupled to the 0th order and $\sim 30\%$ is attributed to reflective and dissipative losses. The loss strongly depends on the polarization of the light: for parallel polarization it is only $\sim 12\%$. This suggests that most of the loss for perpendicular polarization is due to Fresnel reflection and could easily be reduced by an AR-coating of the relevant surfaces of the holographic transmission grating. Typical power levels are 3.3 mW and 18.1 mW for 0th and 1st order output, respectively, and correspond to a diode current of 85 mA. The angular width (FWHM) of the diffraction efficiency *vs.* the incidence angle is 5.5 degrees.

We would like to point out that using a transmission grating as opposed to using a reflective grating is not essential to our concept but provides two advantages. Firstly, as the laser output is the 0th diffraction order of the grating, its direction is maintained when the angular position of the grating is modified in order to tune the laser wavelength. Secondly, *transmission* gratings provide the possibility to use larger line densities. If *reflective* gratings were to be used the line density would have to be smaller in order to ensure that the injected beam and the 1^{st} order output of the grating are clearly separated in space. This separation is needed in a Littman setup in order to provide access to the first order diffraction beam. For the transmission grating used in our experiment the incident beam and 1st order output beam are almost perpendicular to each other.

The 1st order diffraction output is directly injected into the folded cavity shown in Fig. 3. The input coupler always is a plane-plane mirror with a transmission of 8.0% at 846 nm. It is placed at distance of 32 mm from the grating. The distance between the input coupler and the mirror f_2 typically is 10 mm. For each of the two cavity end mirrors (f_2, f_4) two different focal lengths of $f = 37.5$ mm and $f = \infty$ are available and are selected according to which type of cavity is investigated (see Table 2). All end mirrors have a reflectivity of $R \geq 99.5$ %. For stable and well defined operation of the setup we need to control the resonance frequency of two coupled cavities: firstly, as for external cavity diode lasers, we need to ensure that the distance between mirrors f_2 and f_4 equals the optical distance between the mirror f_2 and the laser diodes rear facet up to an integer multiple of $\lambda/2$. This is

done by fine tuning the position of f_4 by means of a PZT. Secondly, we control the emission frequency of the laser system by fine tuning the position of f_2 by means of a second PZT. If the distance between f_3 and f_4 were chosen to exactly equal the optical distance between f_3 and the rear facet of the laser diode, then fine tuning of f_2 would synchronously tune the resonance frequencies of both cavities and the correct position of f_4 would not depend on the desired emission frequency.

The 0th order output of the grating passes an optical isolator (Gsänger DLI-1, 60 dB). A small fraction of that light is directed towards a nearly confocal cavity with a free spectral range (FSR) of 1.5 GHz, which is used to monitor the single mode operation of the setup. The larger fraction of the light is coupled into a single mode fiber. We use a single mode fiber splitter (GOULD) to overlap the GEECDL laser field with the laser field generated by the external cavity diode laser [9] already mentioned at the beginning of Sect. 4. One of the two outputs of the fiber splitter is used to measure the beat note between the GEECDL and that external cavity diode laser, whereas the other one is used to direct light to a wave meter for an absolute frequency measurement.

4.2 *Comparison of different cavity geometries*

We consecutively realize a setup with the planar, the semi-concentric and the confocal cavity, i.e. type 1, 11, and 6 of Table 2, respectively. To maximize the optical feedback, the angular position of the grating is aligned for maximum 1st order diffraction efficiency. Further, for each geometry the position of the collimating lens and the alignment of the cavity are optimized for minimum laser threshold. The laser diode temperature $T = 13.3\,^{\circ}\mathrm{C}$ is kept the same for all setups. We find the lowest threshold of $I_{TH} = 24.1\,\mathrm{mA}$ at $\lambda = 852\,\mathrm{nm}$ for the confocal geometry. This has to be compared to the threshold current in the absence of optical feedback, which is $I_{TH} = 53.4\,\mathrm{mA}$. The threshold currents for the planar ($I_{TH} = 30.0\,\mathrm{mA}$) and the semi-concentric geometry ($I_{TH} = 30.3\,\mathrm{mA}$) at the same wavelength are considerably larger. We conclude that the confocal geometry provides the largest amount of feedback and hence the best coupling of all three geometries. This agrees with the result of our theoretical discussion. Nevertheless, it should be noted that the laser diode beam is far from being mode matched to the non-planar cavities. This is due to the fact that for a radius of curvature of $R = 75\,\mathrm{mm}$ for the cavity mirrors the intra-cavity focal waist is smaller than the waist of the beam injected into the cavity by about one order of magnitude.

We next investigate the continuous tuning range of the setups. Both end mirrors of the external cavity are moved by means of the PZTs in order to tune the external cavity resonance frequency while simultaneously maintaining the coupled cavity resonance condition. For the planar, the semi-concentric and the confocal geometry a continuous tuning range of 0.7 GHz, 1.5 GHz, and 4.9 GHz at $\lambda = 852\,\mathrm{nm}$ are achieved, respectively. This is comparable to continuous tuning ranges of Littrow lasers and is significantly larger than typical continuous tuning ranges achieved with external cavity diode lasers. Hence, we successfully transferred the large continuous tuning ranges of extended cavity diode lasers to the GEECDL concept. We would also like to point out, that at least for the confocal geometry the continuous tuning range exceeds the FSR of the external cavity, which is $\Delta\nu_{FSR} = \sim 2\,\mathrm{GHz}$.

In a second set of experiments we additionally tune the diode laser current. This drastically enhances the continuous tuning ranges, which we now find to correspond to 4.4 GHz, 19.6 GHz, and 45.1 GHz at $\lambda \approx 850\,\mathrm{nm}$ for the planar, semi-concentric, and confocal geometry, respectively. For the latter two of these geometries the tuning range is now limited by the dynamic range of the PZTs. The modification of the diode laser current necessary to achieve the largest tuning range is 15 mA. These results suggest that the GEECDL may provide a continuous tuning range in excess of those typically achieved by Littrow lasers. We would like to mention that Buch and Kohns [18] achieved 14 GHz continuous tuning range with an external cavity diode laser under equivalent conditions, i.e. when controlling the feedback phase and the laser current.

Ultimately, for maximum continuous tunability, the grating will also have to be tilted during a frequency sweep. Continuous tuning ranges on the order of nanometers may then be possible. We would like to point out that this would not require the mechanical sophistication necessary to set up Littman lasers with nanometer tunability [6].

As a third feature we investigate the overall tunability of the GEECDL. We use the setup, which proved to provide the largest continuous tunability, i.e. the confocal geometry. At constant laser diode temperature the GEECDL can be tuned between 834.1 nm and 870.5 nm. This cannot be achieved with external cavity diode lasers. Hence, again we have been able to transfer an important feature of extended cavity diode lasers to the GEECDL concept.

Finally, we would like to mention that the GEECDL shows the same reliability and easiness of operation that is known from extended cavity diode lasers. Even with our setup, which has not yet been designed for mechanical and thermal stability, we achieve stable single mode operation for $\sim 1\,\mathrm{h}$ without controlling the PZTs or the tilt of the grating or of the mirrors. The coarse frequency can be changed by nanometers within minutes, frequency settings are easily reproduced by controlling the PZTs and the laser frequency typically varies only between two or three neighboring longitudinal modes of the laser diode, when mode jumps are forced by actuation of the PZTs.

4.3 *Beat note between GEECDL and external cavity diode laser*

In order to determine an upper limit for the short-term linewidth of the GEECDL we measure the linewidth of the beat note between the GEECDL and the additional external cavity diode laser mentioned already. External cavity diode lasers are well known to provide coherent radiation with a short-term linewidth on the order of 10 kHz [1], which makes them well suited for this kind of measurement. To eliminate the low frequency drift of the external cavity diode laser its frequency is locked to the cesium D2 line at 852 nm by means of a FM-spectroscopy method. As we are interested in the short-term linewidth we also need to reduce the frequency noise at low Fourier frequencies for the GEECDL. Therefore, we lock the GEECDL to the external cavity diode laser at an

offset frequency of ∼50 MHz. A "balanced" difference frequency detector consisting of a low pass filter with a 3 dB corner frequency of 50 MHz followed by a rectifier is used to generate the error signal from the beat note signal provided by an AC-coupled fast photodiode (New Focus 1601-AC 1 GHz receiver). Balancing is achieved by directly rectifying the AC-coupled photo diode signal and subtracting it from the first rectifiers output. We use a single integrator (6 dB/ocatve) in the feedback loop. Below the unity gain frequency of the servo-loop the noise spectral density of the closed-loop error signal is reduced with respect to the open-loop signal, above unity gain frequency it is increased. We estimate the unity gain frequency of the servo-loop from the Fourier frequency at which the closed-loop noise spectral density of the error signal equals the open loop spectral density. A typical value for this frequency is f_G=380 Hz.

We analyze the beat note with an Agilent 4395A spectrum analyzer. From ten independent measurements we find an average line width (FWHM) for a lorentzian line shape of $\delta f = 63$ kHz at a resolution bandwidth of 30 kHz and a sweep time of 76.3 ms for 801 points within a 10 MHz scan. A typical spectrum is shown in Fig. 6. This linewidth is comparable to the short-term linewidth of external cavity diode lasers and is significantly smaller than that of Littrow lasers (typically few hundred kHz [1]). Hence, this proves that a major goal, i.e. the transfer of the narrow line width from the external cavity diode setup to the new concept, has been accomplished. Modest reduction of the loop gain by ∼30 % increases the average linewidth to ∼85 kHz suggesting that residual frequency noise at low Fourier frequencies ($f \sim 400$ Hz and below) is dominating the linewidth of the beat note. We should mention that the mechanical design of the current setup is aiming at maximum flexibility rather than maximum stability. Hence, a straightforward improvement of the mechanical stability and possibly an enhancement of the cavity finesse should easily provide a significant reduction of GEECDL linewidth. In principle, GEECDLs should be able to achieve the same linewidth as external cavity diode lasers.

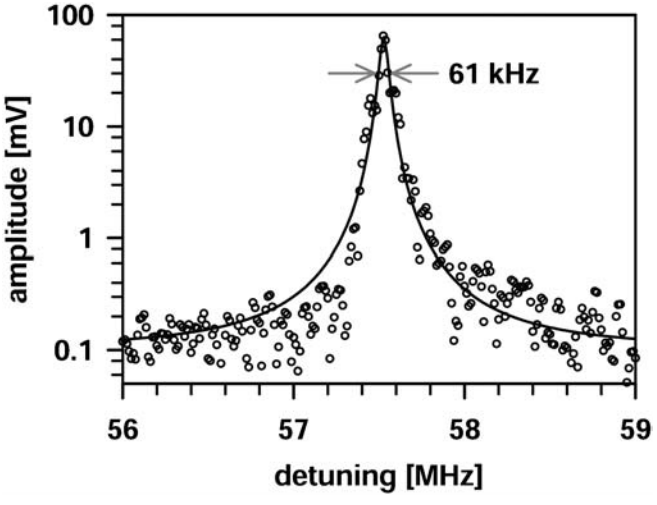

FIGURE 6 Spectrum of the beat note between GEECDL and external cavity diode laser. The FWHM of the lorentzian is 61 kHz. The spectrum analyzer has a resolution bandwidth of 30 kHz, the sweep time is 76.3 ms for 801 points within a 10 MHz span

5 Conclusion

We investigated both theoretically and experimentally a concept for diode lasers with optical feedback. The basic idea is to combine the Littman (extended cavity) and external cavity diode laser setup by replacing the retro mirror of the Littman setup by an external cavity (Grating Enhanced External Cavity Diode Laser, *GEECDL*). The goal is to meet the large overall and continuous tunability, the reliability and easiness of operation known from extended cavity diode lasers with the narrow emission linewidth typical for external cavity diode lasers.

We showed that the proper choice of the external cavity geometry is essential for the GEECDL concept. Among a few hundred possible cavity geometries eleven were found to be most suited for our application. Two of those were determined theoretically to be the most suited geometries: geometry 3 of Table 2 is the least sensitive to a geometry mismatch. Further, it is the only geometry that is not placed at the stability boundary, which is insensitive to a transverse displacement of the cavity with respect to the injected beam. This is important e.g. within the context of thermal drifts. The other geometry, the "confocal" cavity 5, was considered to provide the strongest cavity coupling, which is important e.g. in terms of the tunability of the laser.

Among the eleven geometries mentioned, three were accessible experimentally: the planar 1, the semi-concentric 11, and the confocal geometry 5, of Table 2. The confocal geometry provided the largest continuous tuning range of 45 GHz, which was limited by the dynamic range of the PZTs. The overall tuning range was 36.4 nm at a central wavelength of 852 nm. These results clearly indicate that we successfully transferred the tunability of extended cavity diode lasers to the GEECDL concept. The semi-concentric and the confocal geometry were found to be comparable with respect to reliability and easiness of operation but superseded the planar geometry. However, the confocal geometry clearly provided the lowest threshold. Further, the semi-concentric geometry is placed at the stability boundary so that we expect the confocal geometry to be less sensitive to thermal drifts and mechanical misalignment. Hence, we judge the confocal geometry to provide the best performance among the three geometries investigated experimentally. In order to find an upper limit for the short-term linewidth of the GEECDL we measured the line width of the beat note between a GEECDL with confocal cavity and an external cavity diode laser by means of a fast photo diode and a RF spectrum analyzer. The linewidth of the beat note was found to be ∼60 kHz for a 10 MHz scan of 801 points recorded in 76.3 ms at 30 kHz resolution bandwidth. Taking into account that our setup has yet not been designed for maximum passive stability, we conclude that we also successfully transferred the narrow emission linewidth typical for external cavity diode lasers to the GEECDL concept. In fact, the measurement indicates that the frequency noise was dominated by contributions at low Fourier frequencies (∼400 Hz and below). This suggests that the short-term linewidth of a future GEECDL setup with enhanced cavity finesse and optimized passive stability could be considerably smaller than 60 kHz.

ACKNOWLEDGEMENTS This work was supported by the Deutsche Forschungsgemeinschaft under the grant no. SFB 407.

REFERENCES

1 C.E. Wieman, L. Hollberg: Rev. Sci. Instrum. **62**, l (1991)
2 R. Fox, C. Gates, L. Hollberg: In *Cavity-enhanced spectroscopy*, ed. by R. van Zee, J. Looney (Academic Press, Amsterdam 2002) pp. 1–46
3 W.P. Risk, T. Gosnell, A.V. Nurmikko: *Compact Blue-Green Lasers* (Cambridge University Press, 2003)
4 R. Iffländer: *Solid State Lasers for Material Processing* (Springer Verlag, Berlin 2001)
5 C.J. Myatt, N.R. Newbury, C.E. Wieman: Opt. Lett. **18**, 649 (1993)
6 D. Wandt, M. Laschek, K. Przyklenk, A. Tünnermann, H. Welling: Opt. Commun. **130**, 81 (1996)
7 A. Wolf, B. Bodermann, H.R. Telle: Opt. Lett. **25**, 1098 (2000)
8 M.W. Fleming, A. Mooradian: IEEE J. Quantum Electron. **QE-17**, 44 (1981)
9 B. Dahmani, L. Hollberg, R. Drullinger: Opt. Lett. **12**, 876 (1987)
10 K. Hayasaka: Opt. Commun. **206**, 401 (2002)
11 H. Patrick, C.E. Wieman: Rev. Sci. Instrum. **62**, 2593 (1991)
12 G. Ewald: Staatsexamensarbeit, Universität Mainz (1999); K.-M. Knaak: PhD thesis, Universität Heidelberg (2000)
13 C.H. Henry: IEEE J. Quantum Electron. **QE-18**, 259 (1982)
14 É.M. Belenov, V.L. Velichanskiĭ, A.S. Zibrov, V.V. Nikitin, V.A. Sautenkov, A.V. Uskov: Sov. J. Quantum Electron. **13**, 792 (1983)
15 H. Kogelnik, T. Li: Appl. Optics **5**, 1550 (1966)
16 A.E. Siegman: *Lasers* (University Science Books, Sausalito, CA 1986)
17 Sacher Lasertechnik, private commumcation
18 P. Buch, P. Kohns: IEEE J. Quantum Electron **QE-27**, 1863 (1991)